

<sup>1</sup> **Critical transitions and the fragmenting of global forests**

<sup>2</sup> **Leonardo A. Saravia<sup>1 3</sup>, Santiago R. Doyle<sup>1</sup>, Ben Bond-Lamberty<sup>2</sup>**

<sup>3</sup> 1. Instituto de Ciencias, Universidad Nacional de General Sarmiento, J.M. Gutierrez 1159 (1613), Los  
<sup>4</sup> Polvorines, Buenos Aires, Argentina.

<sup>5</sup> 2. Pacific Northwest National Laboratory, Joint Global Change Research Institute at the University of  
<sup>6</sup> Maryland–College Park, 5825 University Research Court #3500, College Park, MD 20740, USA

<sup>7</sup> 3. Corresponding author e-mail: lsaravia@ungs.edu.ar

<sup>8</sup> **keywords:** Forest fragmentation, early warning signals, percolation, power-laws, MODIS, critical transitions

<sup>9</sup> **Running title:** Critical fragmentation in global forest

<sup>10</sup> **Abstract**

<sup>11</sup> 1. Forests provide critical habitat for many species, essential ecosystem services, and are coupled to  
<sup>12</sup> atmospheric dynamics through exchanges of energy, water and gases. One of the most important  
<sup>13</sup> changes produced in the biosphere is the replacement of forest areas with human dominated landscapes.  
<sup>14</sup> This usually leads to fragmentation, altering the sizes of patches, the structure and function of the  
<sup>15</sup> forest. Here we studied the distribution and dynamics of forest patch sizes at a global level, examining  
<sup>16</sup> signals of a critical transition from an unfragmented to a fragmented state.

<sup>17</sup> 2. We used MODIS vegetation continuous field to estimate the forest patches at a global level and de-  
<sup>18</sup> fined wide regions of connected forest across continents and big islands. We search for critical phase  
<sup>19</sup> transitions, where the system state of the forest changes suddenly at a critical point in time; this  
<sup>20</sup> implies an abrupt change in connectivity that causes an increased fragmentation level. We combined  
<sup>21</sup> five criteria to evaluate the closeness of the system to a fragmentation threshold, studying in particular  
<sup>22</sup> the distribution of forest patch sizes and the dynamics of the largest patch over the last sixteen years.

<sup>23</sup> 3. We found some necessary evidence that allows us to analyze fragmentation as a critical transition:  
<sup>24</sup> all regions followed a power-law distribution over the fifteen years. We also found that the Philip-  
<sup>25</sup> pines region probably went through a critical transition from a fragmented to an unfragmented state.  
<sup>26</sup> Neotropical regions with the highest deforestation rates—South America, Southeast Asia, Africa—all  
<sup>27</sup> met the criteria to be near a critical fragmentation threshold.

<sup>28</sup> 4. This implies that human pressures and climate forcings might trigger undesired effects of fragmentation,  
<sup>29</sup> such as species loss and degradation of ecosystems services, in these regions. The simple criteria  
<sup>30</sup> proposed here could be used as an early warning to estimate the distance to a fragmentation threshold  
<sup>31</sup> in forests around the globe.

## <sup>32</sup> Introduction

<sup>33</sup> Forests are one of the most important biomes on earth, providing habitat for a large proportion of species  
<sup>34</sup> and contributing extensively to global biodiversity (Crowther et al., 2015). In the previous century human  
<sup>35</sup> activities have influenced global bio-geochemical cycles (Bonan, 2008; Canfield, Glazer, & Falkowski, 2010),  
<sup>36</sup> with one of the most dramatic changes being the replacement of 40% of Earth's formerly biodiverse land  
<sup>37</sup> areas with landscapes that contain only a few species of crop plants, domestic animals and humans (J. A.  
<sup>38</sup> Foley et al., 2011). These local changes have accumulated over time and now constitute a global forcing  
<sup>39</sup> (Barnosky et al., 2012). Another global scale forcing that is tied to habitat destruction is fragmentation,  
<sup>40</sup> which is defined as the division of a continuous habitat into separated portions that are smaller and more  
<sup>41</sup> isolated. Fragmentation produces multiple interwoven effects: reductions of biodiversity between 13% and  
<sup>42</sup> 75%, decreasing forest biomass, and changes in nutrient cycling (Haddad et al., 2015). The effects of  
<sup>43</sup> fragmentation are not only important from an ecological point of view but also that of human activities, as  
<sup>44</sup> ecosystem services are deeply influenced by the level of landscape fragmentation (Angelsen, 2010; Mitchell  
<sup>45</sup> et al., 2015; Rudel et al., 2005).

<sup>46</sup> Ecosystems have complex interactions between species and present feedbacks at different levels of organiza-  
<sup>47</sup> tion (Gilman, Urban, Tewksbury, Gilchrist, & Holt, 2010), and external forcings can produce abrupt changes  
<sup>48</sup> from one state to another, called critical transitions (Scheffer et al., 2009). These abrupt state shifts cannot  
<sup>49</sup> be linearly forecasted from past changes, and are thus difficult to predict and manage (Scheffer et al., 2009).  
<sup>50</sup> Such 'critical' transitions have been detected mostly at local scales (S. R. Carpenter et al., 2011; Drake &  
<sup>51</sup> Griffen, 2010), but the accumulation of changes in local communities that overlap geographically can prop-  
<sup>52</sup> agate and theoretically cause an abrupt change of the entire system at larger scales (Barnosky et al., 2012).  
<sup>53</sup> Coupled with the existence of global scale forcings, this implies the possibility that a critical transition could  
<sup>54</sup> occur at a global scale (C. Folke et al., 2011; Rockstrom et al., 2009).

<sup>55</sup> Complex systems can experience two general classes of critical transitions (R V Solé, 2011). In so-called first  
<sup>56</sup> order transitions, a catastrophic regime shift that is mostly irreversible occurs because of the existence of  
<sup>57</sup> alternative stable states (Scheffer et al., 2001). This class of transitions is suspected to be present in a variety  
<sup>58</sup> of ecosystems such as lakes, woodlands, coral reefs (Scheffer et al., 2001), semi-arid grasslands (Brandon T.  
<sup>59</sup> Bestelmeyer et al., 2011), and fish populations (Vasilakopoulos & Marshall, 2015). They can be the result of  
<sup>60</sup> positive feedback mechanisms (Villa Martín, Bonachela, Levin, & Muñoz, 2015); for example, fires in some  
<sup>61</sup> forest ecosystems were more likely to occur in previously burned areas than in unburned places (Kitzberger,  
<sup>62</sup> Aráoz, Gowda, Mermoz, & Morales, 2012).

63 The other class of critical transitions are continuous or second order transitions (Ricard V. Solé & Bas-  
64 compte, 2006). In these cases, there is a narrow region where the system suddenly changes from one domain  
65 to another, with the change being continuous and in theory reversible. This kind of transitions were sug-  
66 gested to be present in tropical forests (S. Pueyo et al., 2010), semi-arid mountain ecosystems (McKenzie  
67 & Kennedy, 2012), and tundra shrublands (Naito & Cairns, 2015). The transition happens at a critical  
68 point where we can observe a distinctive spatial pattern: scale invariant fractal structures characterized by  
69 power law patch distributions (Stauffer & Aharony, 1994). There are several processes that can convert a  
70 catastrophic transition to a second order transitions (Villa Martín et al., 2015). These include stochasticity,  
71 such as demographic fluctuations, spatial heterogeneities, and/or dispersal limitation. All these components  
72 are present in forest around the globe (Filotas et al., 2014; Fung, O'Dwyer, Rahman, Fletcher, & Chisholm,  
73 2016; Seidler & Plotkin, 2006), and thus continuous transitions might be more probable than catastrophic  
74 transitions. Moreover there is some evidence of recovery in some systems that supposedly suffered an irre-  
75 versible transition produced by overgrazing (Brandon T Bestelmeyer, Duniway, James, Burkett, & Havstad,  
76 2013; J. Y. Zhang, Wang, Zhao, Xie, & Zhang, 2005) and desertification (Allington & Valone, 2010).

77 The spatial phenomena observed in continuous critical transitions deal with connectivity, a fundamental  
78 property of general systems and ecosystems from forests (Ochoa-Quintero, Gardner, Rosa, de Barros Ferraz,  
79 & Sutherland, 2015) to marine ecosystems (Leibold & Norberg, 2004) and the whole biosphere (Lenton &  
80 Williams, 2013). When a system goes from a fragmented to a connected state we say that it percolates (R  
81 V Solé, 2011). Percolation implies that there is a path of connections that involves the whole system. Thus  
82 we can characterize two domains or phases: one dominated by short-range interactions where information  
83 cannot spread, and another in which long range interactions are possible and information can spread over  
84 the whole area. (The term “information” is used in a broad sense and can represent species dispersal or  
85 movement.) Thus, there is a critical “percolation threshold” between the two phases, and the system could  
86 be driven close to or beyond this point by an external force; climate change and deforestation are the main  
87 forces that could be the drivers of such a phase change in contemporary forests (Bonan, 2008; Haddad et al.,  
88 2015). There are several applications of this concept in ecology: species’ dispersal strategies are influenced by  
89 percolation thresholds in three-dimensional forest structure (Ricard V Solé, Bartumeus, & Gamarra, 2005),  
90 and it has been shown that species distributions also have percolation thresholds (He & Hubbell, 2003).  
91 This implies that pushing the system below the percolation threshold could produce a biodiversity collapse  
92 (J. Bascompte & Solé, 1996; Pardini, Bueno, Gardner, Prado, & Metzger, 2010; Ricard V. Solé, Alonso, &  
93 Saldaña, 2004); conversely, being in a connected state (above the threshold) could accelerate the invasion of  
94 forest into prairie (Loehle, Li, & Sundell, 1996; Naito & Cairns, 2015).

95 One of the main challenges with systems that can experience critical transitions—of any kind—is that the  
96 value of the critical threshold is not known in advance. In addition, because near the critical point a small  
97 change can precipitate a state shift of the system, they are difficult to predict. Several methods have been  
98 developed to detect if a system is close to the critical point, e.g. a deceleration in recovery from perturbations,  
99 or an increase in variance in the spatial or temporal pattern (Boettiger & Hastings, 2012; S. R. Carpenter  
100 et al., 2011; Dai, Vorselen, Korolev, & Gore, 2012; Hastings & Wysham, 2010).

101 The existence of a critical transition between two states has been established for forest at global scale in  
102 different works (Hirotा, Holmgren, Nes, & Scheffer (2011); Verbesselt et al. (2016); Staal, Dekker, Xu, &  
103 Nes (2016); Wuyts, Champneys, & House (2017)). It is generally believed that this constitutes a first order  
104 catastrophic transition. The regions where forest can grow are not distributed homogeneously, as there  
105 are demographic fluctuations in forest growth and disturbances produced by human activities. Due to new  
106 theoretical advances (Villa Martín, Bonachela, & Muñoz, 2014; Villa Martín et al., 2015) all these factors  
107 imply that if these were first order transitions they will be converted or observed as second order continuous  
108 transitions. From this basis we applied indices derived from second order transitions to global forest cover  
109 dynamics.

110 In this study, our objective is to look for evidence that forests around the globe are near continuous critical  
111 points that represent a fragmentation threshold. We use the framework of percolation to first evaluate if  
112 forest patch distribution at a continental scale is described by a power law distribution and then examine  
113 the fluctuations of the largest patch. The advantage of using data at a continental scale is that for very  
114 large systems the transitions are very sharp (R V Solé, 2011) and thus much easier to detect than at smaller  
115 scales, where noise can mask the signals of the transition.

## 116 Methods

### 117 Study areas definition

118 We analyzed mainland forests at a continental scale, covering the whole globe, by delimiting land areas with  
119 a near-contiguous forest cover, separated with each other by large non-forested areas. Using this criterion,  
120 we delimited the following forest regions. In America, three regions were defined: South America temperate  
121 forest (SAT), subtropical and tropical forest up to Mexico (SAST), and USA and Canada forest (NA). Europe  
122 and North Asia were treated as one region (EUAS). The rest of the delimited regions were South-east Asia  
123 (SEAS), Africa (AF), and Australia (OC). We also included in the analysis islands larger than  $10^5 \text{ km}^2$ . The  
124 mainland region has the number 1 e.g. OC1, and the nearby islands have consecutive numeration (Appendix

125 S4, figure S1-S6). We applied this criterion to delimit regions because we based our study on percolation  
126 theory that assumes some kind of connectivity in the study area (see below).

## 127 Forest patch distribution

128 We studied forest patch distribution in each defined area from 2000 to 2015 using the MODerate-resolution  
129 Imaging Spectroradiometer (MODIS) Vegetation Continuous Fields (VCF) Tree Cover dataset version 051  
130 (C. DiMiceli et al., 2015). This dataset is produced at a global level with a 231-m resolution, from 2000  
131 onwards on an annual basis, the last available year was 2015. There are several definition of forest based  
132 on percent tree cover (J. O. Sexton et al., 2015); we choose a range from 20% to 30% threshold in 5%  
133 increments to convert the percentage tree cover to a binary image of forest and non-forest pixels. This range  
134 is centered in the definition used by the United Nations' International Geosphere-Biosphere Programme  
135 (Belward, 1996), and studies of global fragmentation (Haddad et al., 2015) and includes the range used in  
136 other studies of critical transitions (Xu et al., 2016). Using this range we try to avoid the errors produced  
137 by low discrimination of MODIS VCF between forest and dense herbaceous vegetation at low forest cover  
138 and the saturation of MODIS VCF in dense forests (J. O. Sexton et al., 2013). We repeat all the analysis  
139 for this set of thresholds, except in some specific cases described below. Patches of contiguous forest were  
140 determined in the binary image by grouping connected forest pixels using a neighborhood of 8 forest units  
141 (Moore neighborhood). The MODIS VCF product defines the percentage of tree cover by pixel, but does  
142 not discriminate the type of trees so besides natural forest it includes plantations of tree crops like rubber,  
143 oil palm, eucalyptus and other managed stands (M. Hansen et al., 2014).

## 144 Percolation theory

145 A more in-depth introduction to percolation theory can be found elsewhere (Stauffer & Aharony, 1994) and  
146 a review from an ecological point of view is available (B. Oborny, Szabó, & Meszéna, 2007). Here, to explain  
147 the basic elements of percolation theory we formulate a simple model: we represent our area of interest by a  
148 square lattice and each site of the lattice can be occupied—e.g. by forest—with a probability  $p$ . The lattice  
149 will be more occupied when  $p$  is greater, but the sites are randomly distributed. We are interested in the  
150 connection between sites, so we define a neighborhood as the eight adjacent sites surrounding any particular  
151 site. The sites that are neighbors of other occupied sites define a patch. When there is a patch that connects  
152 the lattice from opposite sides, it is said that the system percolates. When  $p$  is increased from low values, a  
153 percolating patch suddenly appears at some value of  $p$  called the critical point  $p_c$ .

154 Thus percolation is characterized by two well defined phases: the unconnected phase when  $p < p_c$  (called  
155 subcritical in physics), in which species cannot travel far inside the forest, as it is fragmented; in a general  
156 sense, information cannot spread. The second is the connected phase when  $p > p_c$  (supercritical), species  
157 can move inside a forest patch from side to side of the area (lattice), i.e. information can spread over the  
158 whole area. Near the critical point several scaling laws arise: the structure of the patch that spans the area  
159 is fractal, the size distribution of the patches is power-law, and other quantities also follow power-law scaling  
160 (Stauffer & Aharony, 1994).

161 The value of the critical point  $p_c$  depends on the geometry of the lattice and on the definition of the  
162 neighborhood, but other power-law exponents only depend on the lattice dimension. Close to the critical  
163 point, the distribution of patch sizes is:

164 (1)  $n_s(p_c) \propto s^{-\alpha}$

165 where  $n_s(p)$  is the number of patches of size  $s$ . The exponent  $\alpha$  does not depend on the details of the  
166 model and it is called universal (Stauffer & Aharony, 1994). These scaling laws can be applied for landscape  
167 structures that are approximately random, or at least only correlated over short distances (Gastner, Oborny,  
168 Zimmermann, & Pruessner, 2009). In physics this is called “isotropic percolation universality class”, and  
169 corresponds to an exponent  $\alpha = 2.05495$ . If we observe that the patch size distribution has another exponent  
170 it will not belong to this universality class and some other mechanism should be invoked to explain it.  
171 Percolation thresholds can also be generated by models that have some kind of memory (Hinrichsen, 2000;  
172 Ódor, 2004): for example, a patch that has been exploited for many years will recover differently than a  
173 recently deforested forest patch. In this case, the system could belong to a different universality class, or in  
174 some cases there is no universality, in which case the value of  $\alpha$  will depend on the parameters and details  
175 of the model (Corrado, Cherubini, & Pennetta, 2014).

176 To illustrate these concepts, we conducted simulations with a simple forest model with only two states: forest  
177 and non-forest. This type of model is called a “contact process” and was introduced for epidemics (Harris,  
178 1974), but has many applications in ecology (Gastner et al., 2009; Ricard V. Solé & Bascompte, 2006). A  
179 site with forest can become extinct with probability  $e$ , and produce another forest site in a neighborhood  
180 with probability  $c$ . We use a neighborhood defined by an isotropic power law probability distribution. We  
181 defined a single control parameter as  $\lambda = c/e$  and ran simulations for the subcritical fragmentation state  
182  $\lambda < \lambda_c$ , with  $\lambda = 2$ , near the critical point for  $\lambda = 2.5$ , and for the supercritical state with  $\lambda = 5$  (see  
183 supplementary data, gif animations).

184 **Patch size distributions**

185 We fitted the empirical distribution of forest patches calculated for each of the thresholds on the range  
186 we previously mentioned. We used maximum likelihood (Clauset, Shalizi, & Newman, 2009; Goldstein,  
187 Morris, & Yen, 2004) to fit four distributions: power-law, power-law with exponential cut-off, log-normal,  
188 and exponential. We assumed that the patch size distribution is a continuous variable that was discretized  
189 by the remote sensing data acquisition procedure.

190 We set a minimal patch size ( $X_{min}$ ) at nine pixels to fit the patch size distributions to avoid artifacts at patch  
191 edges due to discretization (Weerman et al., 2012). Besides this hard  $X_{min}$  limit we set due to discretization,  
192 the power-law distribution needs a lower bound for its scaling behavior. This lower bound is also estimated  
193 from the data by maximizing the Kolmogorov-Smirnov (KS) statistic, computed by comparing the empirical  
194 and fitted cumulative distribution functions (Clauset et al., 2009). For the log-normal model we constrain  
195 the values of the  $\mu$  parameter to positive values, this parameter controls the mode of the distribution and  
196 when is negative most of the probability density of the distribution lies outside the range of the forest patch  
197 size data (Limpert, Stahel, & Abbt, 2001).

198 To select the best model we calculated corrected Akaike Information Criteria ( $AIC_c$ ) and Akaike weights for  
199 each model (Burnham & Anderson, 2002). Akaike weights ( $w_i$ ) are the weight of evidence in favor of model  
200  $i$  being the actual best model given that one of the  $N$  models must be the best model for that set of  $N$   
201 models. Additionally, we computed a likelihood ratio test (Clauset et al., 2009; Vuong, 1989) of the power  
202 law model against the other distributions. We calculated bootstrapped 95% confidence intervals (Crawley,  
203 2012) for the parameters of the best model, using the bias-corrected and accelerated (BCa) bootstrap (Efron  
204 & Tibshirani, 1994) with 10000 replications.

205 **Largest patch dynamics**

206 The largest patch is the one that connects the highest number of sites in the area. This has been used  
207 extensively to indicate fragmentation (R. H. Gardner & Urban, 2007; Ochoa-Quintero et al., 2015). The  
208 relation of the size of the largest patch  $S_{max}$  to critical transitions has been extensively studied in relation to  
209 percolation phenomena (Bazant, 2000; Botet & Ploszajczak, 2004; Stauffer & Aharony, 1994), but is seldom  
210 used in ecological studies (for an exception see Gastner et al. (2009)). When the system is in a connected  
211 state ( $p > p_c$ ) the landscape is almost insensitive to the loss of a small fraction of forest, but close to the  
212 critical point a minor loss can have important effects (B. Oborny et al., 2007; Ricard V. Solé & Bascompte,  
213 2006), because at this point the largest patch will have a filamentary structure, i.e. extended forest areas

214 will be connected by thin threads. Small losses can thus produce large fluctuations.

215 One way to evaluate the fragmentation of the forest is to calculate the proportion of the largest patch  
216 against the total area (T. H. Keitt, Urban, & Milne, 1997). The total area of the regions we are considering  
217 (Appendix S4, figures S1-S6) may not be the same than the total area that the forest could potentially occupy,  
218 and thus a more accurate way to evaluate the weight of  $S_{max}$  is to use the total forest area, which can be  
219 easily calculated by summing all the forest pixels. We calculate the proportion of the largest patch for each  
220 year, dividing  $S_{max}$  by the total forest area of the same year:  $RS_{max} = S_{max} / \sum_i S_i$ . This has the effect of  
221 reducing the  $S_{max}$  fluctuations produced due to environmental or climatic changes influences in total forest  
222 area. When the proportion  $RS_{max}$  is large (more than 60%) the largest patch contains most of the forest so  
223 there are fewer small forest patches and the system is probably in a connected phase. Conversely, when it is  
224 low (less than 20%), the system is probably in a fragmented phase (Saravia & Momo, 2017). To define if a  
225 region will be in a connected or unconnected state we used the  $RS_{max}$  of the highest (i.e., most conservative)  
226 threshold of 40%, that represent the most dense area of forest within our chosen range. We assume that  
227 there are two alternative states for the critical transition—the forest could be fragmented or unfragmented.  
228 If  $RS_{max}$  is a good indicator of the fragmentation state of the forest its distribution of frequencies should be  
229 bimodal (Brandon T. Bestelmeyer et al., 2011), so we apply the Hartigan's dip test that measures departures  
230 from unimodality (J. A. Hartigan & Hartigan, 1985).

231 The  $RS_{max}$  is a useful qualitative index that does not tell us if the system is near or far from the critical  
232 transition; this can be evaluated using the temporal fluctuations. We calculate the fluctuations around the  
233 mean with the absolute values  $\Delta S_{max} = S_{max}(t) - \langle S_{max} \rangle$ , using the proportions of  $RS_{max}$ . To characterize  
234 fluctuations we fitted three empirical distributions: power-law, log-normal, and exponential, using the same  
235 methods described previously. We expect that large fluctuation near a critical point have heavy tails (log-  
236 normal or power-law) and that fluctuations far from a critical point have exponential tails, corresponding to  
237 Gaussian processes (Rooij, Nash, Rajaraman, & Holden, 2013). As the data set spans 16 years, it is probable  
238 that will do not have enough power to reliably detect which distribution is better (Clauset et al., 2009). To  
239 improve this we used the same likelihood ratio test we used previously (Clauset et al., 2009; Vuong, 1989);  
240 if the p-value obtained to compare the best distribution against the others we concluded that there is not  
241 enough data to decide which is the best model. We generated animated maps showing the fluctuations of  
242 the two largest patches at 30% threshold, to aid in the interpretations of the results.

243 A robust way to detect if the system is near a critical transition is to analyze the increase in variance of the  
244 density (Benedetti-Cecchi, Tamburello, Maggi, & Bulleri, 2015). It has been demonstrated that the variance  
245 increase in density appears when the system is very close to the transition (Corrado et al., 2014), and thus

practically it does not constitute an early warning indicator. An alternative is to analyze the variance of the fluctuations of the largest patch  $\Delta S_{max}$ : the maximum is attained at the critical point but a significant increase occurs well before the system reaches the critical point (Corrado et al., 2014; Saravia & Momo, 2017). In addition, before the critical fragmentation, the skewness of the distribution of  $\Delta S_{max}$  should be negative, implying that fluctuations below the average are more frequent. We characterized the increase in the variance using quantile regression: if variance is increasing the slopes of upper or/and lower quartiles should be positive or negative.

All statistical analyses were performed using the GNU R version 3.3.0 (R Core Team, 2015), to fit the distributions of patch sizes we used the Python package powerlaw (Alstott, Bullmore, & Plenz, 2014). For the quantile regressions we used the R package quantreg (Koenker, 2016). Image processing was done in MATLAB r2015b (The Mathworks Inc.). The complete source code for image processing and statistical analysis, and the patch size data files are available at figshare <http://dx.doi.org/10.6084/m9.figshare.4263905>.

## Results

The figure 1 shows an example of the distribution of the biggest 200 patches for years 2000 and 2014. This distribution is highly variable; the biggest patch usually maintains its spatial location, but sometimes it breaks and then big fluctuations in its size are observed, as we will analyze below. Smaller patches can merge or break more easily so they enter or leave the list of 200, and this is why there is a color change across years.

The power law distribution was selected as the best model in 99% of the cases (Figure S7). In a small number of cases (1%) the power law with exponential cutoff was selected, but the value of the parameter  $\alpha$  was similar by  $\pm 0.03$  to the pure power law (Table S1, and model fit data table). Additionally the patch size where the exponential tail begins is very large, and thus we used the power law parameters for these cases (region EUAS3,SAST2). In finite-size systems the favored model should be the power law with exponential cut-off, because the power-law tails are truncated to the size of the system (Stauffer & Aharony, 1994). This implies that differences between the two kinds of power law models should be small. We observe this effect: when the pure power-law model is selected as the best model the likelihood ratio test shows that in 64% of the cases the differences with power law with exponential cutoff are not significant ( $p\text{-value}>0.05$ ); in these cases the differences between the fitted  $\alpha$  for both models are less than 0.001. Instead the likelihood ratio test clearly differentiates the power law model from the exponential model (100% cases  $p\text{-value}<0.05$ ), and the log-normal model (90% cases  $p\text{-value}<0.05$ ).

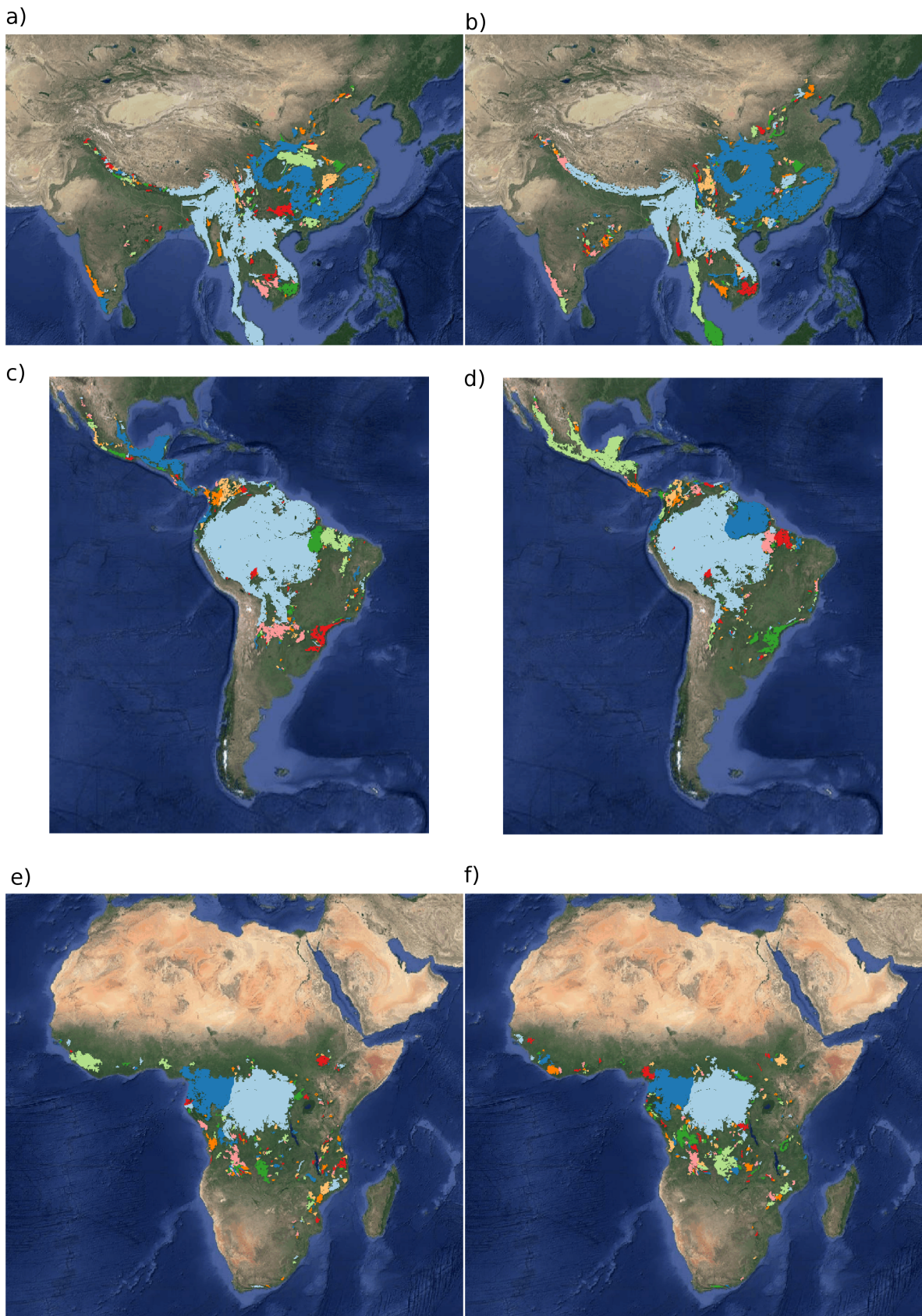


Figure 1: Forest patch distributions for continental regions for the years 2000 and 2014. The images are the 200 biggest patches, shown at a coarse pixel scale of 2.5 km. The regions are: a) & b) southeast Asia; c) & d) South America subtropical and tropical and e) & f) Africa mainland, for the years 2000 and 2014 respectively. The color palette was chosen to discriminate different patches and does not represent patch size.

276 The global mean of the power-law exponent  $\alpha$  is 1.967 and the bootstrapped 95% confidence interval is  
 277 1.964 - 1.970. The global values for each threshold are different, because their confidence intervals do not  
 278 overlap, and their range goes from 1.90 to 2.01 (Table S1). Analyzing the biggest regions (Figure 1, Table  
 279 S2) the northern hemisphere regions (EUAS1 & NA1) have similar values of  $\alpha$  (1.97, 1.98), pantropical areas  
 280 have different  $\alpha$  with greatest values for South America (SAST1, 2.01) and in descending order Africa (AF1,  
 281 1.946) and Southeast Asia (SEAS1, 1.895). With greater  $\alpha$  the fluctuations of patch sizes are lower and vice  
 282 versa (M. E. J. Newman, 2005).

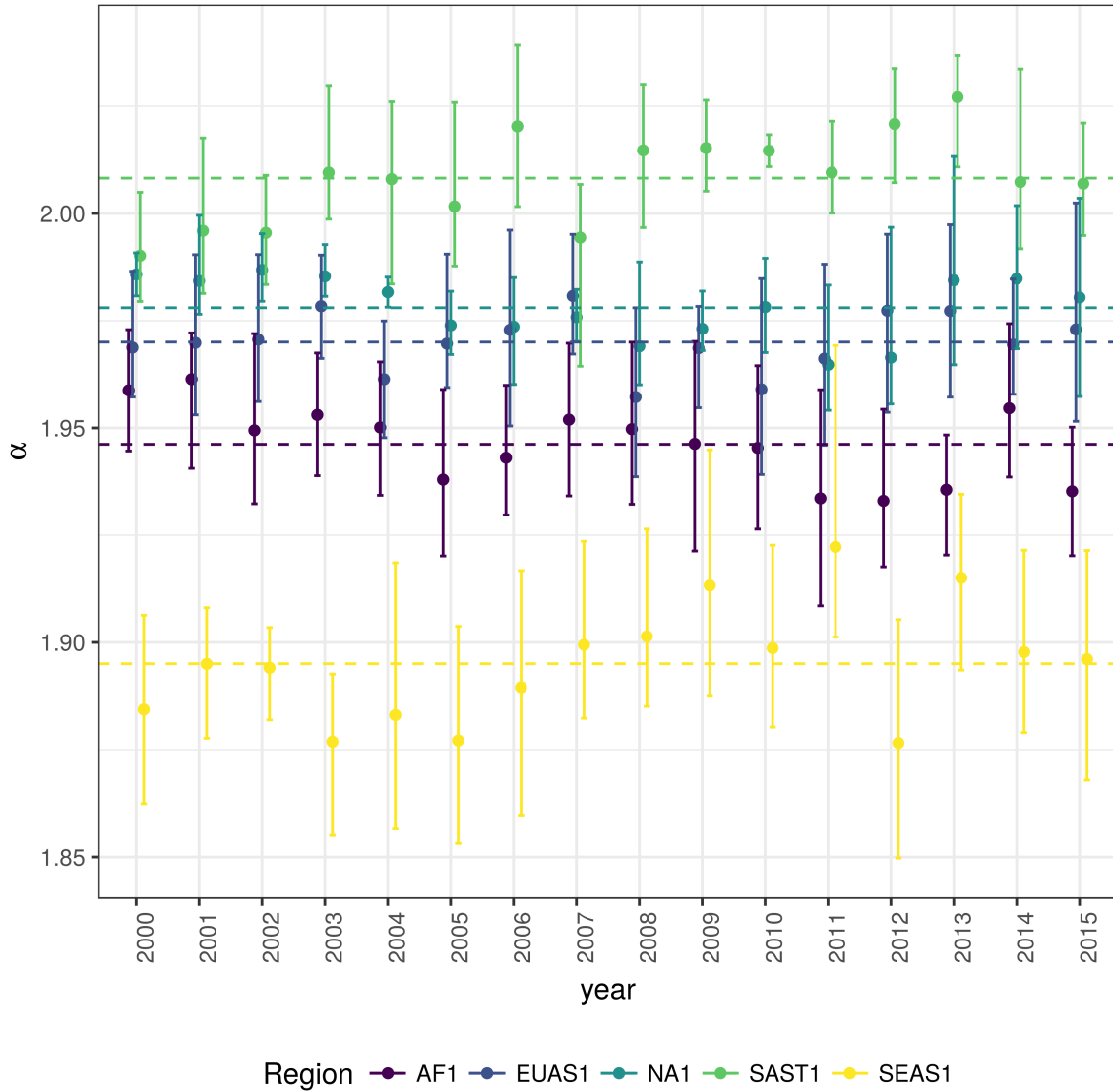


Figure 2: Power law exponents ( $\alpha$ ) of forest patch distributions for regions with total forest area  $> 10^7$  km $^2$ . Dashed horizontal lines are the means by region, with 95% confidence interval error bars estimated by bootstrap resampling. The regions are AF1: Africa mainland, EUAS1: Eurasia mainland, NA1: North America mainland, SAST1: South America subtropical and tropical, SEAS1: Southeast Asia mainland.

We calculated the total areas of forest and the largest patch  $S_{max}$  by year for different thresholds, and as expected these two values increase for smaller thresholds (Table S3). We expect fewer variations in the largest patch relative to total forest area  $RS_{max}$  (Figure S9); in ten cases it stayed near or higher than 60% (EUAS2, NA5, OC2, OC3, OC4, OC5, OC6, OC8, SAST1, SAT1) over the 25-35 range or more. In four cases it stayed around 40% or less, at least over the 25-30% range (AF1, EUAS3, OC1, SAST2), and in six cases there is a crossover from more than 60% to around 40% or less (AF2, EUAS1, NA1, OC7, SEAS1, SEAS2). This confirms the criteria of using the most conservative threshold value of 40% to interpret  $RS_{max}$  with regard to the fragmentation state of the forest. The frequency of  $RS_{max}$  showed bimodality (Figure 3) and the dip test rejected unimodality ( $D = 0.0416$ ,  $p$ -value = 0.0003), which also implies that  $RS_{max}$  is a good index to study the fragmentation state of the forest.

The  $RS_{max}$  for regions with more than  $10^7 \text{ km}^2$  of forest is shown in figure 4. South America tropical and subtropical (SAST1) is the only region with an average close to 60%, the other regions are below 30%. Eurasia mainland (EUAS1) has the lowest value near 20%. For regions with less total forest area (Figure S10, Table S3), Great Britain (EUAS3) has the lowest proportion less than 5%, Java (OC7) and Cuba (SAST2) are under 25%, while other regions such as New Guinea (OC2), Malaysia/Kalimantan (OC3), Sumatra (OC4), Sulawesi (OC5) and South New Zealand (OC6) have a very high proportion (75% or more). Philippines (SEAS2) seems to be a very interesting case because it seems to be under 30% until the year 2007, fluctuates around 30% in years 2008-2010, then jumps near 60% in 2011-2013 and then falls again to 30%, this seems an example of a transition from a fragmented state to a unfragmented one (figure S10).

We analyzed the distributions of fluctuations of the largest patch relative to total forest area  $\Delta RS_{max}$  and the fluctuations of the largest patch  $\Delta S_{max}$ . Although the Akaike criteria identified different distributions as the best, in most cases the Likelihood ratio test was not significant and we are not able, from these data, to determine with confidence which is the best distribution. In only one case was the distribution selected by the Akaike criteria confirmed as the correct model for relative and absolute fluctuations (Table S4).

The animations of the two largest patches (see supplementary data, largest patch gif animations) qualitatively shows the nature of fluctuations and if the state of the forest is connected or not. If the largest patch is always the same patch over time, the forest is probably not fragmented; this happens for regions with  $RS_{max}$  of more than 40% such as AF2 (Madagascar), EUAS2 (Japan), NA5 (Newfoundland) and OC3 (Malaysia). In regions with  $RS_{max}$  between 40% and 30% the identity of the largest patch could change or stay the same in time. For OC7 (Java) the largest patch changes and for AF1 (Africa mainland) it stays the same. Only for EUAS1 (Eurasia mainland) did we observe that the two largest patches are always the same, implying that this region is probably composed of two independent domains and should be sub-divided in future studies.

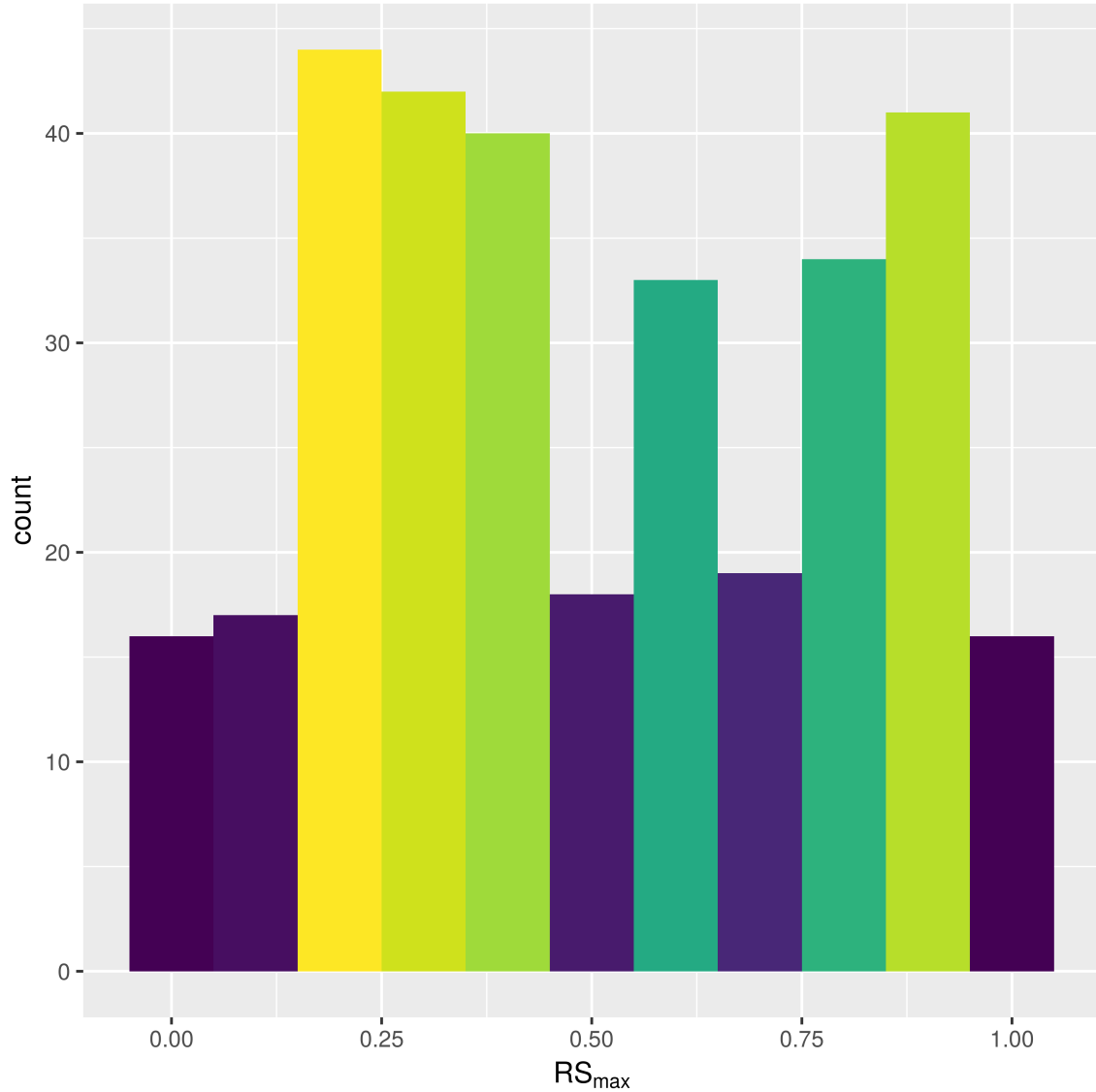


Figure 3: Frequency distribution of Largest patch proportion relative to total forest area  $RS_{max}$  calculated using a threshold of 40% of forest in each pixel to determine patches. Bimodality is observed and confirmed by the dip test ( $D = 0.0416$ ,  $p\text{-value} = 0.0003$ ). This indicates the existence of two states needed for a critical transition.

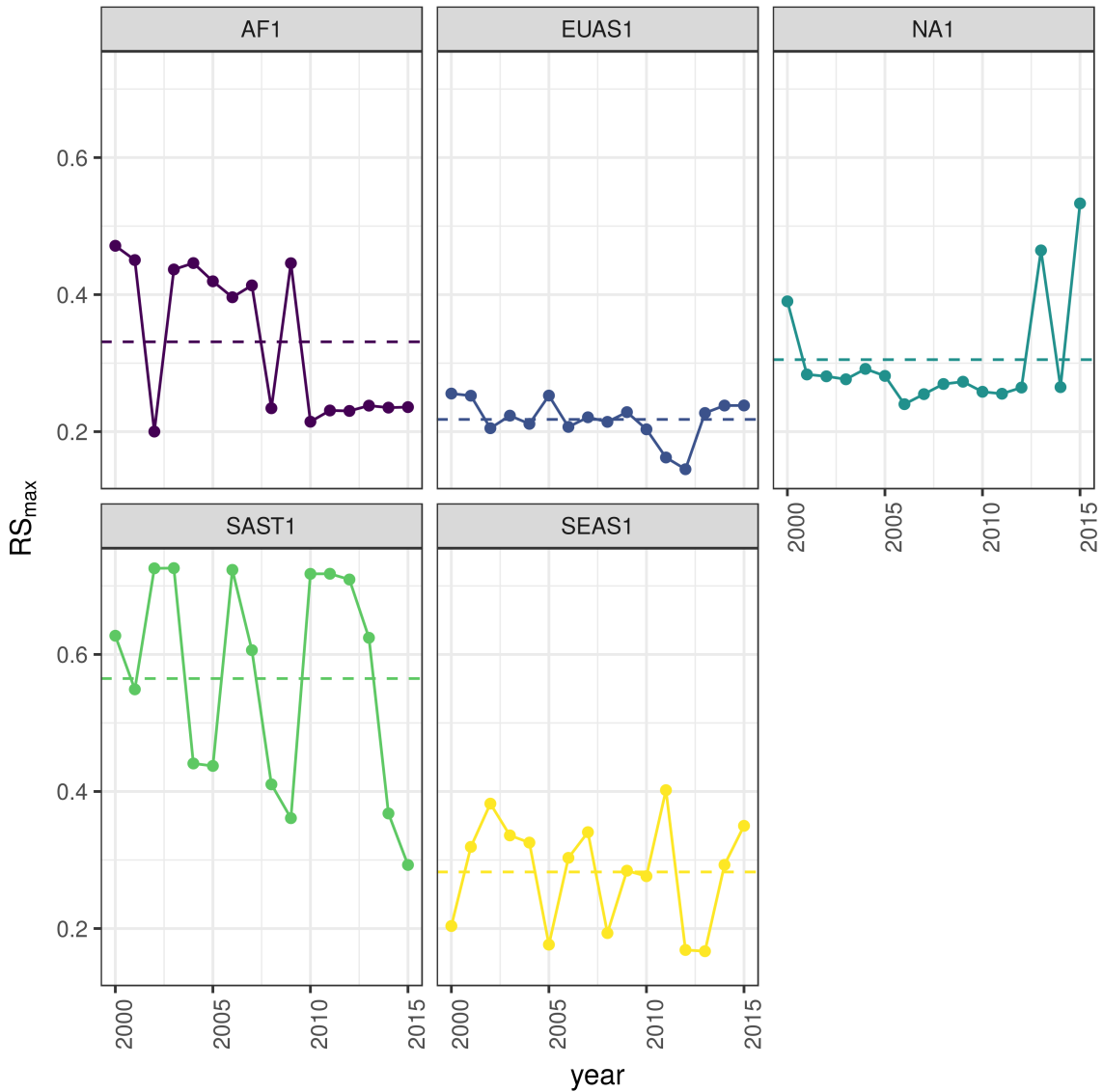


Figure 4: Largest patch proportion relative to total forest area  $RS_{max}$ , for regions with total forest area  $> 10^7 \text{ km}^2$ . We show here the  $RS_{max}$  calculated using a threshold of 40% of forest in each pixel to determine patches. Dashed lines are averages across time. The regions are AF1: Africa mainland, EUAS1: Eurasia mainland, NA1: North America mainland, SAST1: South America tropical and subtropical, SEAS1: Southeast Asia mainland.

315 The regions with  $RS_{max}$  less than 25% included SAST2 (Cuba) and EUAS3 (Great Britain); in these cases  
316 the always-changing largest patch reflects their fragmented state. In the case of SEAS2 (Philippines) a  
317 transition is observed, with the identity of the largest patch first variable, and then constant after 2010.

318 The results of quantile regressions are almost identical for  $\Delta RS_{max}$  and  $\Delta S_{max}$  (table S5). Among the biggest  
319 regions, Africa (AF1) has a similar pattern across thresholds but only the 30% threshold is significant; the  
320 upper and lower quantiles have significant negative slopes, but the lower quantile slope is lower, implying  
321 that negative fluctuations and variance are increasing (Figure 5). Eurasia mainland (EUAS1) has significant  
322 slopes at 20%, 30% and 40% thresholds but the patterns are different at 20% variance is decreasing, at  
323 30% and 40% only is increasing. Thus the variation of the most dense portion of the largest patch is  
324 increasing within a limited range. North America mainland (NA1) exhibits the same pattern at 20%, 25%  
325 and 30% thresholds: a significant lower quantile with positive slope, implying decreasing variance. South  
326 America tropical and subtropical (SAST1) have significant lower quantile with negative slope at 25% and 30%  
327 thresholds indicating an increase in variance. SEAS1 has an upper quantile with positive slope significant  
328 for 25% threshold, also indicating an increasing variance. The other regions, with forest area smaller than  
329  $10^7 \text{ km}^2$  are shown in figure S11 and table S5. Philippines (SEAS2) is an interesting case: the slopes of lower  
330 quantiles are positive for thresholds 20% and 25%, and the upper quantile slopes are positive for thresholds  
331 30% and 40%; thus variance is decreasing at 20%-25% and increasing at 30%-40%.

332 The conditions that indicate that a region is near a critical fragmentation threshold are that patch size  
333 distributions follow a power law; variance of  $\Delta RS_{max}$  is increasing in time; and skewness is negative. All  
334 these conditions must happen at the same time at least for one threshold. When the threshold is higher more  
335 dense regions of the forest are at risk. This happens for Africa mainland (AF1), Eurasia mainland(EUAS1),  
336 Japan (EUAS2), Australia mainland (OC1), Malaysia/Kalimantan (OC3), Sumatra (OC4), South America  
337 tropical & subtropical (SAST1), Cuba (SAST2), Southeast Asia, Mainland (SEAS1).

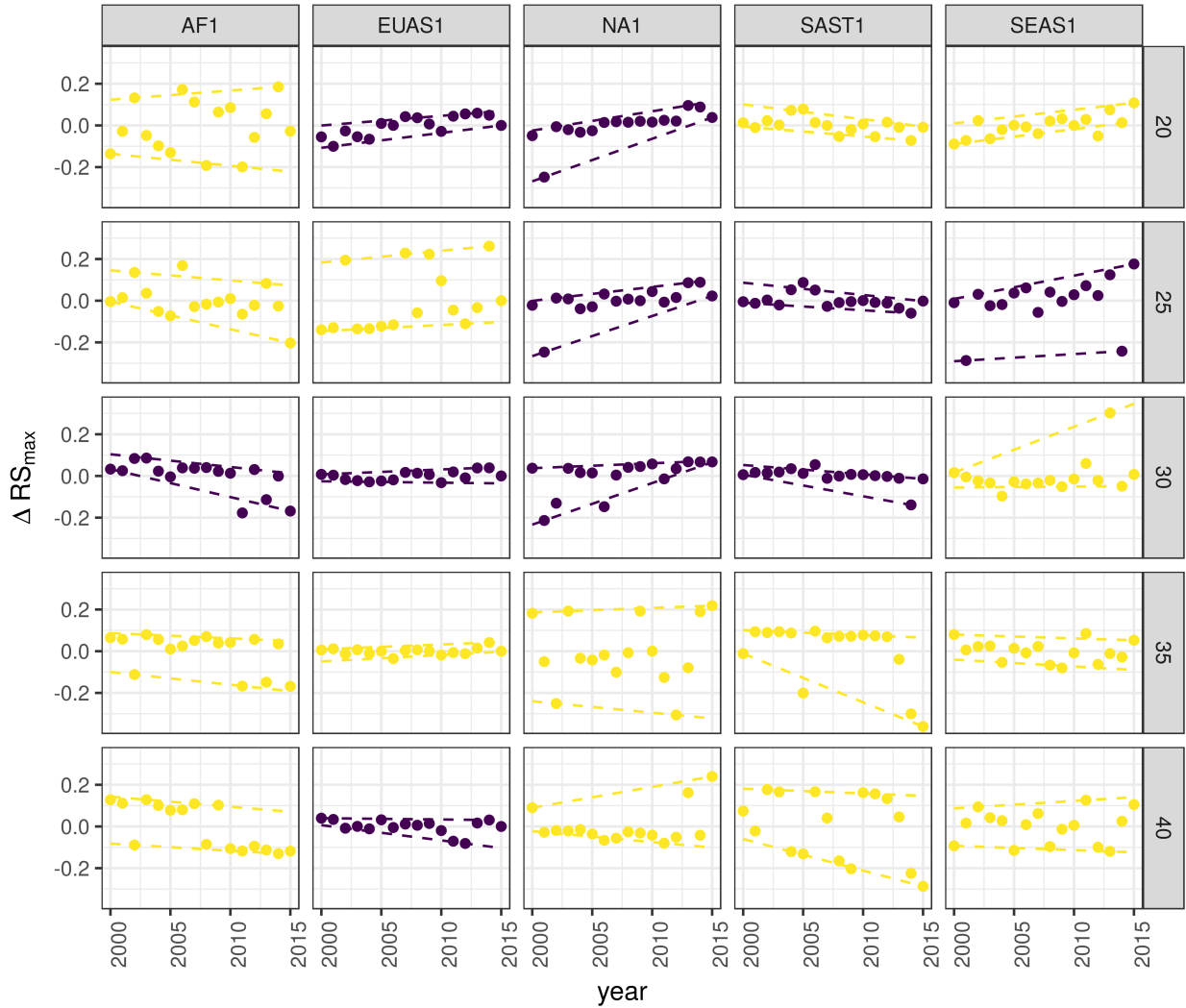


Figure 5: Largest patch fluctuations for regions with total forest area  $> 10^7 \text{ km}^2$  across years. The patch sizes are relative to the total forest area of the same year. Dashed lines are 90% and 10% quantile regressions, to show if fluctuations were increasing; purple (dark) panels have significant slopes. The regions are AF1: Africa mainland, EUAS1: Eurasia mainland, NA1: North America mainland, SAST1: South America tropical and subtropical, SEAS1: Southeast Asia mainland.

Table 1: Regions and indicators of closeness to a critical fragmentation point. Where:  $RS_{max}$  is the largest patch divided by the total forest area; Threshold is the value used to calculate patches from the MODIS VCF pixels;  $\Delta RS_{max}$  are the fluctuations of  $RS_{max}$  around the mean and the increase or decrease in the variance was estimated using quantile regressions; skewness was calculated for  $RS_{max}$ . NS means the results were non-significant. The conditions that determine the closeness to a fragmentation point are: increasing variance of  $\Delta RS_{max}$  and negative skewness.  $RS_{max}$  indicates if the forest is unfragmented ( $>0.6$ ) or fragmented ( $<0.3$ ).

Region	Description	$RS_{max}$	Threshold	Variance of $\Delta RS_{max}$	Skewness
AF1	Africa mainland	0.33	30	Increase	-1.4653
AF2	Madagascar	0.48	20	Increase	0.7226
EUAS1	Eurasia, mainland	0.22	20	Decrease	-0.4814
EUAS1			30	Increase	0.3113
EUAS1			40	Increase	-1.2790
EUAS2	Japan	0.94	35	Increase	-0.3913
EUAS2			40	Increase	-0.5030
EUAS3	Great Britain	0.03	40	NS	
NA1	North America, mainland	0.31	20	Decrease	-2.2895
NA1			25	Decrease	-2.4465
NA1			30	Decrease	-1.6340
NA5	Newfoundland	0.54	40	NS	
OC1	Australia, Mainland	0.36	30	Increase	0.0920
OC1			35	Increase	-0.8033
OC2	New Guinea	0.96	25	Decrease	-0.1003
OC2			30	Decrease	0.1214
OC2			35	Decrease	-0.0124
OC3	Malaysia/Kalimantan	0.92	35	Increase	-1.0147
OC3			40	Increase	-1.5649
OC4	Sumatra	0.84	20	Increase	-1.3846
OC4			25	Increase	-0.5887
OC4			30	Increase	-1.4226
OC5	Sulawesi	0.82	40	NS	
OC6	New Zealand South Island	0.75	40	Increase	0.3553
OC7	Java	0.16	40	NS	
OC8	New Zealand North Island	0.64	40	NS	
SAST1	South America, Tropical and Subtropical forest	0.56	25	Increase	1.0519
SAST1			30	Increase	-2.7216
SAST2	Cuba	0.15	20	Increase	0.5049
SAST2			25	Increase	1.7263
SAST2			30	Increase	0.1665
SAST2			40	Increase	-0.5401
SAT1	South America, Temperate forest	0.54	25	Decrease	0.1483
SAT1			30	Decrease	-1.6059
SAT1			35	Decrease	-1.3809
SEAS1	Southeast Asia, Mainland	0.28	25	Increase	-1.3328
SEAS2	Philippines	0.33	20	Decrease	-1.6373
SEAS2			25	Decrease	-0.6648
SEAS2			30	Increase	0.1517

Region	Description	$RS_{max}$	Threshold	Variance of $\Delta RS_{max}$	Skewness
SEAS2			40	Increase	1.5996

## 338 Discussion

339 We found that the forest patch distribution of all regions of the world, spanning tropical rainforests, boreal  
 340 and temperate forests, followed power laws spanning seven orders of magnitude. Power laws have previously  
 341 been found for several kinds of vegetation, but never at global scales as in this study. Moreover the range  
 342 of the estimated power law exponents is relatively narrow (1.90 - 2.01), even though we tested a variety  
 343 of different thresholds levels. This suggest the existence of one unifying mechanism, or perhaps different  
 344 mechanisms that act in the same way in different regions, affecting forest spatial structure and dynamics.

345 Several mechanisms have been proposed for the emergence of power laws in forests. The first is related  
 346 self organized criticality (SOC), when the system is driven by its internal dynamics to a critical state; this  
 347 has been suggested mainly for fire-driven forests (Hantson, Pueyo, & Chuvieco, 2015; Zinck & Grimm,  
 348 2009). Real ecosystems do not seem to meet the requirements of SOC dynamics (McKenzie & Kennedy,  
 349 2012; S. Pueyo et al., 2010), however, because they have both endogenous and exogenous controls, are non-  
 350 homogeneous, and do not have a separation of time scales [Ricard V Solé, Alonso, & Mckane (2002); Sole2006].

351 A second possible mechanism, suggested by Pueyo et al. (2010), is isotropic percolation: when a system is  
 352 near the critical point, the power law structures arise. This is equivalent to the random forest model that  
 353 we explained previously, and requires the tuning of an external environmental condition to carry the system  
 354 to this point. We did not expect forest growth to be a random process at local scales, but it is possible that  
 355 combinations of factors cancel out to produce seemingly random forest dynamics at large scales. In this case  
 356 we should have observed power laws in a limited set of situations that coincide with a critical point, but  
 357 instead we observed pervasive power law distributions. Thus isotopic percolation does not seem likely to be  
 358 the mechanism that produces the observed distributions. A third possible mechanism is facilitation (Irvine,  
 359 Bull, & Keeling, 2016; Manor & Shnerb, 2008): a patch surrounded by forest will have a smaller probability  
 360 of being deforested or degraded than an isolated patch. The model of Scanlon et al. (2007) showed an  
 361  $\alpha = 1.34$  which is different from our results (1.90 - 2.01 range). Another model but with three states  
 362 (tree/non-tree/degraded), including local facilitation and grazing, was also used to obtain power laws patch  
 363 distributions without external tuning, and exhibited deviations from power laws at high grazing pressures  
 364 (S. Kéfi et al., 2007). The values of the power law exponent  $\alpha$  obtained for this model are dependent on the  
 365 intensity of facilitation: when facilitation is more intense the exponent is higher, but the maximal values they

366 obtained are still lower than the ones we observed. The interesting point is that the value of the exponent is  
367 dependent on the parameters, and thus the observed  $\alpha$  might be obtained with some parameter combination.

368 The existence of possible critical transitions in forests, mainly in neotropical forest to savanna, is a matter  
369 of intense investigation, with the transitions generally thought to be first order or discontinuous transitions.

370 Here, however, we found power laws in forest patch distributions, implying (i.e., a necessary but not a  
371 sufficient condition) a second order or continuous transition. A power law patch distribution can be indicative  
372 of a critical transition if it is present in a narrow range of conditions; conversely, if it is not found, the existence  
373 of a critical transition cannot be discarded. New research (Villa Martín et al., 2014, 2015) has suggested  
374 that first order transitions do not even exist when the system is (i) spatially heterogeneous and (ii) exhibits  
375 internal and external stochastic fluctuations, as in forests. Thus the application of indices based on second  
376 order transitions seems to be justified.

377 It has been suggested that a combination of spatial and temporal indicators could more reliably detect  
378 critical transitions (S. Kéfi et al., 2014). In this study, we combined five criteria to evaluate the closeness  
379 of the system to a fragmentation threshold. Two of them were spatial: the forest patch size distribution,  
380 and the proportion of the largest patch relative to total forest area  $RS_{max}$ . The other three were the  
381 distribution of temporal fluctuations in the largest patch size, the trend in the variance, and the skewness  
382 of the fluctuations. One of them: the distribution of temporal fluctuations  $\Delta RS_{max}$  can not be applied  
383 with our temporal resolution due to the difficulties of fitting and comparing heavy tailed distributions. The  
384 combination of the remaining four gives us an increased degree of confidence about the system being close  
385 to a critical transition.

386 Monitoring the biggest patches using  $RS_{max}$  is also important regardless of the existence or not of critical  
387 transitions.  $RS_{max}$  is relative to total forest area thus it could be used to compare regions with a different  
388 extension of forests and as the total area of forest also changes with different environmental conditions,  
389 e.g. this could be used to compare forest from different latitudes. Moreover, the areas covered by  $S_{max}$   
390 across regions contain most of the intact forest landscapes defined by P. Potapov et al. (2008), and thus  
391  $RS_{max}$  is a relatively simple way to evaluate the risk in these areas.

392 This analysis is at scale of continents so it is in fact a macrosystems analysis (Heffernan et al., 2014), in  
393 which it is important to link local processes with resulting larger-scale (here, continental) patterns. Here, we  
394 identified macro-scale dynamical patterns that deserve attention. To link these patterns across scales requires  
395 a substantial amount of investigation, probably performing the same analysis for smaller regions that identify  
396 more clearly which kind of forest and processes are locally involved. We know that the same procedure could

397 be applied to local scales because the patch distributions are power laws; power law distributions are self-  
398 similar, or invariant to scale changes. Thus unless power law distribution are broken we could apply the  
399 same methodology to more local scales.

400 South America tropical and subtropical (SAST1), Southeast Asia mainland (SEAS1) and Africa mainland  
401 (AF1) met all criteria at least for one threshold; these regions generally experience the biggest rates of  
402 deforestation with a significant increase in loss of forest (M. C. Hansen et al., 2013). From our point of view  
403 the most critical region is Southeast Asia, because the proportion of the largest patch relative to total forest  
404 area  $RS_{max}$  was 28%. This suggests that Southeast Asia's forests are the most fragmented, and thus its  
405 flora and fauna the most endangered. Due to the criteria we adopted to define regions, we could not detect  
406 the effect of conservation policies applied at a country level, e.g. the Natural Forest Conservation Program  
407 in China, which has produced an 1.6% increase in forest cover and net primary productivity over the last  
408 20 years (Viña, McConnell, Yang, Xu, & Liu, 2016). Indonesia and Malaysia (OC3) both are countries with  
409 hight deforestation rates (M. C. Hansen et al., 2013); Sumatra (OC4) is the biggest island of Indonesia and  
410 where most deforestation occurs. Both regions show a high  $RS_{max}$  greater than 60%, and thus the forest is  
411 in an unfragmented state, but they met all other criteria, meaning that they are approaching a transition if  
412 the actual deforestation rates continue. At present our indices are qualitative but we expect to develop them  
413 in a more quantitative way to predict how many years would be needed to complete a critical transition if  
414 actual forest loss rates are maintained.

415 The Eurasian mainland region (EUAS1) is an extensive area with mainly temperate and boreal forest, and a  
416 combination of forest loss due to fire (P. Potapov, Hansen, Stehman, Loveland, & Pittman, 2008) and forestry.  
417 The biggest country is Russia that experienced the biggest rate of forest loss of all countries, but here in  
418 the zone of coniferous forest the the largest gain is observed due to agricultural abandonment (Prishchepov,  
419 Müller, Dubinin, Baumann, & Radeloff, 2013). The loss is maximum at the most dense areas of forest (M.  
420 C. Hansen et al., 2013, Table S3), this coincides with our analysis that detect an increasing risk at denser  
421 forest. This region also has a relatively low  $RS_{max}$  that means is probably near a fragmented state. A region  
422 that is similar in forest composition to EAUS1 is North America (NA1); the two main countries involved,  
423 United States and Canada, have forest dynamics mainly influenced by fire and forestry, with both regions are  
424 extensively managed for industrial wood production. North America has a higher  $RS_{max}$  than Eurasia and  
425 a positive skewness that excludes it from being near a critical transition. A possible explanation of this is  
426 that in Russia after the collapse of the Soviet Union harvest was lower due to agricultural abandonment but  
427 illegal overharvesting of high valued stands has increased in recent decades (Gauthier, Bernier, Kuuluvainen,  
428 Shvidenko, & Schepaschenko, 2015).

429 The analysis of  $RS_{max}$  reveals that the island of Philippines (SEAS2) seems to be an example of a critical  
430 transition from an unconnected to a connected state, i.e. from a state with high fluctuations and low  $RS_{max}$   
431 to a state with low fluctuations and high  $RS_{max}$ . If we observe this pattern backwards in time, the decrease  
432 in variance increases, and negative skewness is constant, and thus the region exhibits the criteria of a critical  
433 transition (Table 1, Figure S11). The actual pattern of transition to an unfragmented state could be the  
434 result of an active intervention of the government promoting conservation and rehabilitation of protected  
435 areas, ban of logging old-growth forest, reforestation of barren areas, community-based forestry activities,  
436 and sustainable forest management in the country's production forest (Lasco et al., 2008). This confirms  
437 that the early warning indicators proposed here work in the correct direction. An important caveat is that  
438 the MODIS dataset does not detect if native forest is replaced by agroindustrial tree plantations like oil  
439 palms, that are among the main drivers of deforestation in this area (Malhi, Gardner, Goldsmith, Silman, &  
440 Zelazowski, 2014). To improve the estimation of forest patches, data sets as the MODIS cropland probability  
441 and others about land use, protected areas, forest type, should be incorporated (M. Hansen et al., 2014; J.  
442 O. Sexton et al., 2015).

443 Deforestation and fragmentation are closely related. At low levels of habitat reduction species population  
444 will decline proportionally; this can happen even when the habitat fragments retain connectivity. As habitat  
445 reduction continues, the critical threshold is approached and connectivity will have large fluctuations (Brook,  
446 Ellis, Perring, Mackay, & Blomqvist, 2013). This could trigger several negative synergistic effects: population  
447 fluctuations and the possibility of extinctions will rise, increasing patch isolation and decreasing connectivity  
448 (Brook et al., 2013). This positive feedback mechanism will be enhanced when the fragmentation threshold is  
449 reached, resulting in the loss of most habitat specialist species at a landscape scale (Pardini et al., 2010). Some  
450 authors have argued that since species have heterogeneous responses to habitat loss and fragmentation, and  
451 biotic dispersal is limited, the importance of thresholds is restricted to local scales or even that its existence  
452 is questionable (Brook et al., 2013). Fragmentation is by definition a local process that at some point  
453 produces emergent phenomena over the entire landscape, even if the area considered is infinite (B. Oborny,  
454 Meszéna, & Szabó, 2005). In addition, after a region's fragmentation threshold connectivity decreases, there  
455 is still a large and internally well connected patch that can maintain sensitive species (A. C. Martensen,  
456 Ribeiro, Banks-Leite, Prado, & Metzger, 2012). What is the time needed for these large patches to become  
457 fragmented, and pose a real danger of extinction to a myriad of sensitive species? If a forest is already in  
458 a fragmented state, a second critical transition from forest to non-forest could happen: the desertification  
459 transition (Corrado et al., 2014). Considering the actual trends of habitat loss, and studying the dynamics  
460 of non-forest patches—instead of the forest patches as we did here—the risk of this kind of transition could

461 be estimated. The simple models proposed previously could also be used to estimate if these thresholds are  
462 likely to be continuous and reversible or discontinuous and often irreversible (Weissmann & Shnerb, 2016),  
463 and the degree of protection (e.g. using the set-asides strategy Banks-Leite et al. (2014)) that would be  
464 necessary to stop this trend.

465 The effectiveness of landscape management is related to the degree of fragmentation, and the criteria to  
466 direct reforestation efforts could be focused on regions near a transition (B. Oborny et al., 2007). Regions  
467 that are in an unconnected state require large efforts to recover a connected state, but regions that are near  
468 a transition could be easily pushed to a connected state; feedbacks due to facilitation mechanisms might  
469 help to maintain this state. Crossing the fragmentation critical point in forests could have negative effects  
470 on biodiversity and ecosystem services (Haddad et al., 2015), but it could also produce feedback loops at  
471 different levels of the biological hierarchy. This means that a critical transition produced at a continental  
472 scale could have effects at the level of communities, food webs, populations, phenotypes and genotypes  
473 (Barnosky et al., 2012). All these effects interact with climate change, thus there is a potential production of  
474 cascading effects that could lead to an abrupt climate change with potentially large ecological and economic  
475 impact (Alley et al., 2003).

476 Therefore, even if critical thresholds are reached only in some forest regions at a continental scale, a cascading  
477 effect with global consequences could still be produced (Reyer, Rammig, Brouwers, & Langerwisch, 2015).  
478 The risk of such event will be higher if the dynamics of separate continental regions are coupled (Lenton  
479 & Williams, 2013). At least three of the regions defined here are considered tipping elements of the earth  
480 climate system that could be triggered during this century (Lenton et al., 2008). These were defined as policy  
481 relevant tipping elements so that political decisions could determine whether the critical value is reached or  
482 not. Thus using the criteria proposed here could be used as a more sensitive system to evaluate the closeness  
483 of a tipping point at a continental scale, but the same criteria could also be used to evaluate local problems  
484 at smaller areas. Further improvements will produce quantitative predictions about the temporal horizon  
485 where these critical transitions could produce significant changes in the studied systems.

## 486 Supporting information

### 487 Appendix

488 *Table S1:* Mean power-law exponent and Bootstrapped 95% confidence intervals by threshold.

489 *Table S2:* Mean power-law exponent and Bootstrapped 95% confidence intervals across thresholds by region  
490 and year.

491 *Table S3:* Mean total patch area; largest patch  $S_{max}$  in km<sup>2</sup>; largest patch proportional to total patch area  
 492  $RS_{max}$  and 95% bootstrapped confidence interval of  $RS_{max}$ , by region and thresholds, averaged across years

493 *Table S4:* Model selection for distributions of fluctuation of largest patch  $\Delta S_{max}$  and largest patch relative  
 494 to total forest area  $\Delta RS_{max}$ .

495 *Table S5:* Quantil regressions of the fluctuations of the largest patch vs year, for 10% and 90% quantils at  
 496 different pixel thresholds.

497 *Table S6:* Unbiased estimation of Skewness of fluctuations of the largest patch  $\Delta S_{max}$  and fluctuations  
 498 relative to total forest area  $\Delta RS_{max}$ .

499 *Figure S1:* Regions for Africa: Mainland (AF1), Madagascar (AF2).

500 *Figure S2:* Regions for Eurasia: Mainland (EUAS1), Japan (EUAS2), Great Britain (EUAS3).

501 *Figure S3:* Regions for North America: Mainland (NA1), Newfoundland (NA5).

502 *Figure S4:* Regions for Australia and islands: Australia mainland (OC1), New Guinea (OC2),  
 503 Malaysia/Kalimantan (OC3), Sumatra (OC4), Sulawesi (OC5), New Zealand south island (OC6),  
 504 Java (OC7), New Zealand north island (OC8).

505 *Figure S5:* Regions for South America: Tropical and subtropical forest up to Mexico (SAST1), Cuba  
 506 (SAST2), South America Temperate forest (SAT1).

507 *Figure S6:* Regions for Southeast Asia: Mainland (SEAS1), Philippines (SEAS2).

508 *Figure S7:* Proportion of best models selected for patch size distributions using the Akaike criterion.

509 *Figure S8:* Power law exponents for forest patch distributions by year for all regions.

510 *Figure S9:* Average largest patch relative to total forest area  $RS_{max}$  by threshold, for all regions.

511 *Figure S10:* Largest patch relative to total forest area  $RS_{max}$  by year at 40% threshold, for regions with  
 512 total forest area less than 10<sup>7</sup> km<sup>2</sup>.

513 *Figure S11:* Fluctuations of largest patch relative to total forest area  $RS_{max}$  for regions with total forest  
 514 area less than 10<sup>7</sup> km<sup>2</sup> by year and threshold.

## 515 **Data Accessibility**

516 The MODIS VCF product is freely available from NASA at <https://search.earthdata.nasa.gov/>. Csv text file  
 517 with model fits for patch size distribution, and model selection for all the regions; Gif Animations of a forest

518 model percolation; Gif animations of largest patches; patch size files for all years and regions used here; and all  
519 the R, Python and Matlab scripts are available at figshare <http://dx.doi.org/10.6084/m9.figshare.4263905>.

520 **Acknowledgments**

521 LAS and SRD are grateful to the National University of General Sarmiento for financial support. We want to  
522 thank to Jordi Bascompte, Nara Guisoni, Fernando Momo, and two anonymous reviewers for their comments  
523 and discussions that greatly improved the manuscript. This work was partially supported by a grant from  
524 CONICET (PIO 144-20140100035-CO).

525 **References**

- 526 Alley, R. B., Marotzke, J., Nordhaus, W. D., Overpeck, J. T., Peteet, D. M., Pielke, R. A., ... Wallace, J. M.  
527 (2003). Abrupt Climate Change. *Science*, 299(5615), 2005–2010. Retrieved from <http://science.sciencemag.org/content/299/5615/2005.abstract>
- 529 Allington, G. R. H., & Valone, T. J. (2010). Reversal of desertification: The role of physical and chemical  
530 soil properties. *Journal of Arid Environments*, 74(8), 973–977. doi:10.1016/j.jaridenv.2009.12.005
- 531 Alstott, J., Bullmore, E., & Plenz, D. (2014). powerlaw: A Python Package for Analysis of Heavy-Tailed  
532 Distributions. *PLOS ONE*, 9(1), e85777. Retrieved from <https://doi.org/10.1371/journal.pone.0085777>
- 533 Angelsen, A. (2010). Policies for reduced deforestation and their impact on agricultural production. *Pro-*  
534 *ceedings of the National Academy of Sciences*, 107(46), 19639–19644. doi:10.1073/pnas.0912014107
- 535 Banks-Leite, C., Pardini, R., Tambosi, L. R., Pearse, W. D., Bueno, A. A., Bruscagin, R. T., ... Metzger,  
536 J. P. (2014). Using ecological thresholds to evaluate the costs and benefits of set-asides in a biodiversity  
537 hotspot. *Science*, 345(6200), 1041–1045. doi:10.1126/science.1255768
- 538 Barnosky, A. D., Hadly, E. A., Bascompte, J., Berlow, E. L., Brown, J. H., Fortelius, M., ... Smith, A. B.  
539 (2012). Approaching a state shift in Earth’s biosphere. *Nature*, 486(7401), 52–58. doi:10.1038/nature11018
- 540 Bascompte, J., & Solé, R. V. (1996). Habitat fragmentation and extinction threholds in spatially explicit  
541 models. *Journal of Animal Ecology*, 65(4), 465–473. doi:10.2307/5781
- 542 Bazant, M. Z. (2000). Largest cluster in subcritical percolation. *Physical Review E*, 62(2), 1660–1669.  
543 Retrieved from <http://link.aps.org/doi/10.1103/PhysRevE.62.1660>
- 544 Belward, A. S. (1996). *The IGBP-DIS Global 1 Km Land Cover Data Set “DISCover”: Proposal and*

- 545 *Implementation Plans : Report of the Land Recover Working Group of IGBP-DIS* (p. 61). IGBP-DIS Office.
- 546 Retrieved from <https://books.google.com.ar/books?id=qixsNAAACAAJ>
- 547 Benedetti-Cecchi, L., Tamburello, L., Maggi, E., & Bulleri, F. (2015). Experimental Perturbations Mod-
- 548 ify the Performance of Early Warning Indicators of Regime Shift. *Current Biology*, 25(14), 1867–1872.
- 549 doi:10.1016/j.cub.2015.05.035
- 550 Bestelmeyer, B. T., Duniway, M. C., James, D. K., Burkett, L. M., & Havstad, K. M. (2013). A test of
- 551 critical thresholds and their indicators in a desertification-prone ecosystem: more resilience than we thought.
- 552 *Ecology Letters*, 16, 339–345. doi:10.1111/ele.12045
- 553 Bestelmeyer, B. T., Ellison, A. M., Fraser, W. R., Gorman, K. B., Holbrook, S. J., Laney, C. M., ... Sharma,
- 554 S. (2011). Analysis of abrupt transitions in ecological systems. *Ecosphere*, 2(12), 129. doi:10.1890/ES11-
- 555 00216.1
- 556 Boettiger, C., & Hastings, A. (2012). Quantifying limits to detection of early warning for critical transitions.
- 557 *Journal of the Royal Society Interface*, 9(75), 2527–2539. doi:10.1098/rsif.2012.0125
- 558 Bonan, G. B. (2008). Forests and Climate Change: forcings, Feedbacks, and the Climate Benefits of Forests.
- 559 *Science*, 320(5882), 1444–1449. doi:10.1126/science.1155121
- 560 Botet, R., & Ploszajczak, M. (2004). Correlations in Finite Systems and Their Universal Scaling Properties.
- 561 In K. Morawetz (Ed.), *Nonequilibrium physics at short time scales: Formation of correlations* (pp. 445–466).
- 562 Berlin Heidelberg: Springer-Verlag.
- 563 Brook, B. W., Ellis, E. C., Perring, M. P., Mackay, A. W., & Blomqvist, L. (2013). Does the terrestrial
- 564 biosphere have planetary tipping points? *Trends in Ecology & Evolution*. doi:10.1016/j.tree.2013.01.016
- 565 Burnham, K., & Anderson, D. R. (2002). *Model selection and multi-model inference: A practical information-*
- 566 *theoretic approach* (2nd. ed., p. 512). New York: Springer-Verlag.
- 567 Canfield, D. E., Glazer, A. N., & Falkowski, P. G. (2010). The Evolution and Future of Earth's Nitrogen
- 568 Cycle. *Science*, 330(6001), 192–196. doi:10.1126/science.1186120
- 569 Carpenter, S. R., Cole, J. J., Pace, M. L., Batt, R., Brock, W. A., Cline, T., ... Weidel, B. (2011).
- 570 Early Warnings of Regime Shifts: A Whole-Ecosystem Experiment. *Science*, 332(6033), 1079–1082.
- 571 doi:10.1126/science.1203672
- 572 Clauset, A., Shalizi, C., & Newman, M. (2009). Power-Law Distributions in Empirical Data. *SIAM Review*,

- 573 51(4), 661–703. doi:10.1137/070710111
- 574 Corrado, R., Cherubini, A. M., & Pennetta, C. (2014). Early warning signals of desertification transitions  
575 in semiarid ecosystems. *Physical Review E - Statistical, Nonlinear, and Soft Matter Physics*, 90(6), 62705.  
576 doi:10.1103/PhysRevE.90.062705
- 577 Crawley, M. J. (2012). *The R Book* (2nd. ed., p. 1076). Hoboken, NJ, USA: Wiley.
- 578 Crowther, T. W., Glick, H. B., Covey, K. R., Bettigole, C., Maynard, D. S., Thomas, S. M., ... Bradford, M.  
579 A. (2015). Mapping tree density at a global scale. *Nature*, 525(7568), 201–205. doi:10.1038/nature14967
- 580 Dai, L., Vorselen, D., Korolev, K. S., & Gore, J. (2012). Generic Indicators for Loss of Resilience Before a  
581 Tipping Point Leading to Population Collapse. *Science*, 336(6085), 1175–1177. doi:10.1126/science.1219805
- 582 DiMiceli, C., Carroll, M., Sohlberg, R., Huang, C., Hansen, M., & Townshend, J. (2015). Annual Global Au-  
583 tomated MODIS Vegetation Continuous Fields (MOD44B) at 250 m Spatial Resolution for Data Years Begin-  
584 ning Day 65, 2000 - 2014, Collection 051 Percent Tree Cover, University of Maryland, College Park, MD, USA.  
585 Retrieved from [https://lpdaac.usgs.gov/dataset{\\\_}discovery/modis/modis{\\\_}products{\\\_}table/mod44b](https://lpdaac.usgs.gov/dataset{\_}discovery/modis/modis{\_}products{\_}table/mod44b)
- 586 Drake, J. M., & Griffen, B. D. (2010). Early warning signals of extinction in deteriorating environments.  
587 *Nature*, 467(7314), 456–459. doi:10.1038/nature09389
- 588 Efron, B., & Tibshirani, R. J. (1994). *An Introduction to the Bootstrap* (p. 456). New York: Taylor &  
589 Francis. Retrieved from <https://books.google.es/books?id=gLlpIUXRntoC>
- 590 Filotas, E., Parrott, L., Burton, P. J., Chazdon, R. L., Coates, K. D., Coll, L., ... Messier, C. (2014). Viewing  
591 forests through the lens of complex systems science. *Ecosphere*, 5(January), 1–23. doi:10.1890/ES13-00182.1
- 592 Foley, J. A., Ramankutty, N., Brauman, K. A., Cassidy, E. S., Gerber, J. S., Johnston, M., ... Zaks, D. P. M.  
593 (2011). Solutions for a cultivated planet. *Nature*, 478(7369), 337–342. doi:10.1038/nature10452
- 594 Folke, C., Jansson, Å., Rockström, J., Olsson, P., Carpenter, S. R., Iii, F. S. C., ... Westley, F. (2011).  
595 Reconnecting to the Biosphere. *AMBIO*, 40(7), 719–738. doi:10.1007/s13280-011-0184-y
- 596 Fung, T., O'Dwyer, J. P., Rahman, K. A., Fletcher, C. D., & Chisholm, R. A. (2016). Reproducing static  
597 and dynamic biodiversity patterns in tropical forests: the critical role of environmental variance. *Ecology*,  
598 97(5), 1207–1217. doi:10.1890/15-0984.1
- 599 Gardner, R. H., & Urban, D. L. (2007). Neutral models for testing landscape hypotheses. *Landscape Ecology*,  
600 22(1), 15–29. doi:10.1007/s10980-006-9011-4
- 601 Gastner, M. T., Oborny, B., Zimmermann, D. K., & Pruessner, G. (2009). Transition from Connected

- 602 to Fragmented Vegetation across an Environmental Gradient: Scaling Laws in Ecotone Geometry. *The*  
603 *American Naturalist*, 174(1), E23–E39. doi:10.1086/599292
- 604 Gauthier, S., Bernier, P., Kuuluvainen, T., Shvidenko, A. Z., & Schepaschenko, D. G. (2015). Boreal forest  
605 health and global change. *Science*, 349(6250), 819 LP–822. Retrieved from <http://science.sciencemag.org/content/349/6250/819.abstract>
- 606 Gilman, S. E., Urban, M. C., Tewksbury, J., Gilchrist, G. W., & Holt, R. D. (2010). A framework  
607 for community interactions under climate change. *Trends in Ecology & Evolution*, 25(6), 325–331.  
608 doi:10.1016/j.tree.2010.03.002
- 609 Goldstein, M. L., Morris, S. A., & Yen, G. G. (2004). Problems with fitting to the power-law distri-  
610 bution. *The European Physical Journal B - Condensed Matter and Complex Systems*, 41(2), 255–258.  
611 doi:10.1140/epjb/e2004-00316-5
- 612 Haddad, N. M., Brudvig, L. a., Clobert, J., Davies, K. F., Gonzalez, A., Holt, R. D., ... Townshend, J. R.  
613 (2015). Habitat fragmentation and its lasting impact on Earth's ecosystems. *Science Advances*, 1(2), 1–9.  
614 doi:10.1126/sciadv.1500052
- 615 Hansen, M. C., Potapov, P. V., Moore, R., Hancher, M., Turubanova, S. A., Tyukavina, A., ... Townshend,  
616 J. R. G. (2013). High-Resolution Global Maps of 21st-Century Forest Cover Change. *Science*, 342(6160),  
617 850–853. doi:10.1126/science.1244693
- 618 Hansen, M., Potapov, P., Margono, B., Stehman, S., Turubanova, S., & Tyukavina, A. (2014). Response  
619 to Comment on “High-resolution global maps of 21st-century forest cover change”. *Science*, 344(6187), 981.  
620 doi:10.1126/science.1248817
- 621 Hantson, S., Pueyo, S., & Chuvieco, E. (2015). Global fire size distribution is driven by human impact and  
622 climate. *Global Ecology and Biogeography*, 24(1), 77–86. doi:10.1111/geb.12246
- 623 Harris, T. E. (1974). Contact interactions on a lattice. *The Annals of Probability*, 2, 969–988.
- 624 Hartigan, J. A., & Hartigan, P. M. (1985). The Dip Test of Unimodality. *The Annals of Statistics*, 13(1),  
625 70–84. Retrieved from <http://www.jstor.org/stable/2241144>
- 626 Hastings, A., & Wysham, D. B. (2010). Regime shifts in ecological systems can occur with no warning.  
627 *Ecology Letters*, 13(4), 464–472. doi:10.1111/j.1461-0248.2010.01439.x
- 628 He, F., & Hubbell, S. (2003). Percolation Theory for the Distribution and Abundance of Species. *Physical*

- 630 *Review Letters*, 91(19), 198103. doi:10.1103/PhysRevLett.91.198103
- 631 Heffernan, J. B., Soranno, P. A., Angilletta, M. J., Buckley, L. B., Gruner, D. S., Keitt, T. H., ... Weathers,  
632 K. C. (2014). Macrosystems ecology: understanding ecological patterns and processes at continental scales.  
633 *Frontiers in Ecology and the Environment*, 12(1), 5–14. doi:10.1890/130017
- 634 Hinrichsen, H. (2000). Non-equilibrium critical phenomena and phase transitions into absorbing states.  
635 *Advances in Physics*, 49(7), 815–958. doi:10.1080/00018730050198152
- 636 Hirota, M., Holmgren, M., Nes, E. H. V., & Scheffer, M. (2011). Global Resilience of Tropical Forest and  
637 Savanna to Critical Transitions. *Science*, 334(6053), 232–235. doi:10.1126/science.1210657
- 638 Irvine, M. A., Bull, J. C., & Keeling, M. J. (2016). Aggregation dynamics explain vegetation patch-size  
639 distributions. *Theoretical Population Biology*, 108, 70–74. doi:10.1016/j.tpb.2015.12.001
- 640 Keitt, T. H., Urban, D. L., & Milne, B. T. (1997). Detecting critical scales in fragmented landscapes.  
641 *Conservation Ecology*, 1(1), 4. Retrieved from <http://www.ecologyandsociety.org/vol1/iss1/art4/>
- 642 Kéfi, S., Guttal, V., Brock, W. A., Carpenter, S. R., Ellison, A. M., Livina, V. N., ... Dakos, V. (2014).  
643 Early Warning Signals of Ecological Transitions: Methods for Spatial Patterns. *PLoS ONE*, 9(3), e92097.  
644 doi:10.1371/journal.pone.0092097
- 645 Kéfi, S., Rietkerk, M., Alados, C. L., Pueyo, Y., Papanastasis, V. P., ElAich, A., & Ruiter, P. C. de.  
646 (2007). Spatial vegetation patterns and imminent desertification in Mediterranean arid ecosystems. *Nature*,  
647 449(7159), 213–217. doi:10.1038/nature06111
- 648 Kitzberger, T., Aráoz, E., Gowda, J. H., Mermoz, M., & Morales, J. M. (2012). Decreases in Fire Spread  
649 Probability with Forest Age Promotes Alternative Community States, Reduced Resilience to Climate Vari-  
650 ability and Large Fire Regime Shifts. *Ecosystems*, 15(1), 97–112. doi:10.1007/s10021-011-9494-y
- 651 Koenker, R. (2016). quantreg: Quantile Regression. Retrieved from <http://cran.r-project.org/package=quantreg>
- 652 Lasco, R. D., Pulhin, F. B., Cruz, R. V. O., Pulhin, J. M., Roy, S. S. N., & Sanchez, P. A. J. (2008). Forest  
653 responses to changing rainfall in the Philippines. In N. Leary, C. Conde, & J. Kulkarni (Eds.), *Climate  
654 change and vulnerability* (pp. 49–66). London: Earthscan. Retrieved from <http://gen.lib.rus.ec/book/index.php?md5=AD313B13E05C9D61A9EC1EE2E73A91FB>
- 655 Leibold, M. A., & Norberg, J. (2004). Biodiversity in metacommunities: Plankton as complex adaptive

- systems? *Limnology and Oceanography*, 49(4, part 2), 1278–1289. doi:10.4319/lo.2004.49.4\_part\_2.1278
- Lenton, T. M., & Williams, H. T. P. (2013). On the origin of planetary-scale tipping points. *Trends in Ecology & Evolution*, 28(7), 380–382. doi:10.1016/j.tree.2013.06.001
- Lenton, T. M., Held, H., Kriegler, E., Hall, J. W., Lucht, W., Rahmstorf, S., & Schellnhuber, H. J. (2008). Tipping elements in the Earth's climate system. *Proceedings of the National Academy of Sciences*, 105(6), 1786–1793. doi:10.1073/pnas.0705414105
- Limpert, E., Stahel, W. A., & Abbt, M. (2001). Log-normal Distributions across the Sciences: Keys and CluesOn the charms of statistics, and how mechanical models resembling gambling machines offer a link to a handy way to characterize log-normal distributions, which can provide deeper insight into var. *BioScience*, 51(5), 341–352. Retrieved from [http://dx.doi.org/10.1641/0006-3568\(2001\)051\[0341:LNDATS\]2.0.CO](http://dx.doi.org/10.1641/0006-3568(2001)051[0341:LNDATS]2.0.CO)
- Loehle, C., Li, B.-L., & Sundell, R. C. (1996). Forest spread and phase transitions at forest-prairie ecotones in Kansas, U.S.A. *Landscape Ecology*, 11(4), 225–235.
- Malhi, Y., Gardner, T. A., Goldsmith, G. R., Silman, M. R., & Zelazowski, P. (2014). Tropical Forests in the Anthropocene. *Annual Review of Environment and Resources*, 39(1), 125–159. doi:10.1146/annurev-environ-030713-155141
- Manor, A., & Shnerb, N. M. (2008). Origin of pareto-like spatial distributions in ecosystems. *Physical Review Letters*, 101(26), 268104. doi:10.1103/PhysRevLett.101.268104
- Martensen, A. C., Ribeiro, M. C., Banks-Leite, C., Prado, P. I., & Metzger, J. P. (2012). Associations of Forest Cover, Fragment Area, and Connectivity with Neotropical Understory Bird Species Richness and Abundance. *Conservation Biology*, 26(6), 1100–1111. doi:10.1111/j.1523-1739.2012.01940.x
- McKenzie, D., & Kennedy, M. C. (2012). Power laws reveal phase transitions in landscape controls of fire regimes. *Nat Commun*, 3, 726. Retrieved from <http://dx.doi.org/10.1038/ncomms1731> [http://www.nature.com/ncomms/journal/v3/n3/supplinfo/ncomms1731{\\\_\}S1.html](http://www.nature.com/ncomms/journal/v3/n3/supplinfo/ncomms1731{\_\}S1.html)
- Mitchell, M. G. E., Suarez-Castro, A. F., Martinez-Harms, M., Maron, M., McAlpine, C., Gaston, K. J., ... Rhodes, J. R. (2015). Reframing landscape fragmentation's effects on ecosystem services. *Trends in Ecology & Evolution*, 30(4), 190–198. doi:10.1016/j.tree.2015.01.011
- Naito, A. T., & Cairns, D. M. (2015). Patterns of shrub expansion in Alaskan arctic river corridors suggest phase transition. *Ecology and Evolution*, 5(1), 87–101. doi:10.1002/ece3.1341
- Newman, M. E. J. (2005). Power laws, Pareto distributions and Zipf's law. *Contemporary Physics*, 46(5),

- 687 323–351. doi:10.1080/00107510500052444
- 688 Oborny, B., Meszéna, G., & Szabó, G. (2005). Dynamics of Populations on the Verge of Extinction. *Oikos*,  
689 109(2), 291–296. Retrieved from <http://www.jstor.org/stable/3548746>
- 690 Oborny, B., Szabó, G., & Meszéna, G. (2007). Survival of species in patchy landscapes: percolation in  
691 space and time. In *Scaling biodiversity* (pp. 409–440). Cambridge University Press. Retrieved from <http://dx.doi.org/10.1017/CBO9780511814938.022>
- 693 Ochoa-Quintero, J. M., Gardner, T. A., Rosa, I., de Barros Ferraz, S. F., & Sutherland, W. J. (2015).  
694 Thresholds of species loss in Amazonian deforestation frontier landscapes. *Conservation Biology*, 29(2),  
695 440–451. doi:10.1111/cobi.12446
- 696 Ódor, G. (2004). Universality classes in nonequilibrium lattice systems. *Reviews of Modern Physics*, 76(3  
697 I), 663–724. doi:10.1103/RevModPhys.76.663
- 698 Pardini, R., Bueno, A. de A., Gardner, T. A., Prado, P. I., & Metzger, J. P. (2010). Beyond the Fragmen-  
699 tation Threshold Hypothesis: Regime Shifts in Biodiversity Across Fragmented Landscapes. *PLoS ONE*,  
700 5(10), e13666. doi:10.1371/journal.pone.0013666
- 701 Potapov, P., Hansen, M. C., Stehman, S. V., Loveland, T. R., & Pittman, K. (2008). Combining MODIS  
702 and Landsat imagery to estimate and map boreal forest cover loss. *Remote Sensing of Environment*, 112(9),  
703 3708–3719. doi:<https://doi.org/10.1016/j.rse.2008.05.006>
- 704 Potapov, P., Yaroshenko, A., Turubanova, S., Dubinin, M., Laestadius, L., Thies, C., ... Zhuravleva, I. (2008).  
705 Mapping the world's intact forest landscapes by remote sensing. *Ecology and Society*, 13(2).
- 706 Prishchepov, A. V., Müller, D., Dubinin, M., Baumann, M., & Radeloff, V. C. (2013). Determinants  
707 of agricultural land abandonment in post-Soviet European Russia. *Land Use Policy*, 30(1), 873–884.  
708 doi:<https://doi.org/10.1016/j.landusepol.2012.06.011>
- 709 Pueyo, S., de Alencastro Graça, P. M. L., Barbosa, R. I., Cots, R., Cardona, E., & Fearnside, P. M. (2010).  
710 Testing for criticality in ecosystem dynamics: the case of Amazonian rainforest and savanna fire. *Ecology  
711 Letters*, 13(7), 793–802. doi:10.1111/j.1461-0248.2010.01497.x
- 712 R Core Team. (2015). R: A Language and Environment for Statistical Computing. Vienna, Austria: R  
713 Foundation for Statistical Computing. Retrieved from <http://www.r-project.org/>
- 714 Reyer, C. P. O., Rammig, A., Brouwers, N., & Langerwisch, F. (2015). Forest resilience, tipping points and

- 715 global change processes. *Journal of Ecology*, 103(1), 1–4. doi:10.1111/1365-2745.12342
- 716 Rockstrom, J., Steffen, W., Noone, K., Persson, A., Chapin, F. S., Lambin, E. F., ... Foley, J. A. (2009). A  
717 safe operating space for humanity. *Nature*, 461(7263), 472–475. Retrieved from <http://dx.doi.org/10.1038/461472a>
- 718
- 719 Rooij, M. M. J. W. van, Nash, B., Rajaraman, S., & Holden, J. G. (2013). A Fractal Approach to Dynamic  
720 Inference and Distribution Analysis. *Frontiers in Physiology*, 4(1). doi:10.3389/fphys.2013.00001
- 721 Rudel, T. K., Coomes, O. T., Moran, E., Achard, F., Angelsen, A., Xu, J., & Lambin, E. (2005). Forest  
722 transitions: towards a global understanding of land use change. *Global Environmental Change*, 15(1), 23–31.  
723 doi:<https://doi.org/10.1016/j.gloenvcha.2004.11.001>
- 724 Saravia, L. A., & Momo, F. R. (2017). Biodiversity collapse and early warning indicators in  
725 a spatial phase transition between neutral and niche communities. *PeerJ PrePrints*, 5, e1589v4.  
726 doi:10.7287/peerj.preprints.1589v3
- 727 Scanlon, T. M., Caylor, K. K., Levin, S. A., & Rodriguez-iturbe, I. (2007). Positive feedbacks promote  
728 power-law clustering of Kalahari vegetation. *Nature*, 449(September), 209–212. doi:10.1038/nature06060
- 729 Scheffer, M., Bascompte, J., Brock, W. A., Brovkin, V., Carpenter, S. R., Dakos, V., ... Sugihara, G. (2009).  
730 Early-warning signals for critical transitions. *Nature*, 461(7260), 53–59. doi:10.1038/nature08227
- 731 Scheffer, M., Walker, B., Carpenter, S., Foley, J. a, Folke, C., & Walker, B. (2001). Catastrophic shifts in  
732 ecosystems. *Nature*, 413(6856), 591–596. doi:10.1038/35098000
- 733 Seidler, T. G., & Plotkin, J. B. (2006). Seed Dispersal and Spatial Pattern in Tropical Trees. *PLoS Biology*,  
734 4(11), e344. doi:10.1371/journal.pbio.0040344
- 735 Sexton, J. O., Noojipady, P., Song, X.-P., Feng, M., Song, D.-X., Kim, D.-H., ... Townshend, J. R.  
736 (2015). Conservation policy and the measurement of forests. *Nature Climate Change*, 6(2), 192–196.  
737 doi:10.1038/nclimate2816
- 738 Sexton, J. O., Song, X.-P., Feng, M., Noojipady, P., Anand, A., Huang, C., ... Townshend, J. R. (2013).  
739 Global, 30-m resolution continuous fields of tree cover: Landsat-based rescaling of MODIS vegetation con-  
740 tinuous fields with lidar-based estimates of error. *International Journal of Digital Earth*, 6(5), 427–448.  
741 doi:10.1080/17538947.2013.786146
- 742 Solé, R. V. (2011). *Phase Transitions* (p. 223). Princeton University Press. Retrieved from <https://books.google.com/books?id=KUWzDwAAQBAJ&pg=PA223&lpg=PA223&dq=phase+transitions+R+V+Sole&source=bl&ots=ZBxgkLcOOG&sig=9CmzqfzGKuIyfzrJFyfzGKuIyfz&hl=en&sa=X&ved=0ahUKEwiTzq6WzqfUAhVJz4KHSWYDw0Q6wEwC&qid=1481110000000&sr=1&bbc=1&ie=UTF8>

- 743 google.com.ar/books?id=8RcLuv-Ll2kC
- 744 Solé, R. V., & Bascompte, J. (2006). *Self-organization in complex ecosystems* (p. 373). New Jersey, USA.:  
 745 Princeton University Press. Retrieved from <http://books.google.com.ar/books?id=v4gpGH6Gv68C>
- 746 Solé, R. V., Alonso, D., & Mckane, A. (2002). Self-organized instability in complex ecosystems. *Philosophical Transactions of the Royal Society of London. Series B, Biological Sciences*, 357(May), 667–681.  
 747  
 748 doi:10.1098/rstb.2001.0992
- 749 Solé, R. V., Alonso, D., & Saldaña, J. (2004). Habitat fragmentation and biodiversity collapse in neutral  
 750 communities. *Ecological Complexity*, 1(1), 65–75. doi:10.1016/j.ecocom.2003.12.003
- 751 Solé, R. V., Bartumeus, F., & Gamarra, J. G. P. (2005). Gap percolation in rainforests. *Oikos*, 110(1),  
 752 177–185. doi:10.1111/j.0030-1299.2005.13843.x
- 753 Staal, A., Dekker, S. C., Xu, C., & Nes, E. H. van. (2016). Bistability, Spatial Interaction, and the  
 754 Distribution of Tropical Forests and Savannas. *Ecosystems*, 19(6), 1080–1091. doi:10.1007/s10021-016-0011-  
 755 1
- 756 Stauffer, D., & Aharony, A. (1994). *Introduction To Percolation Theory* (p. 179). London: Taylor & Francis.
- 757 Vasilakopoulos, P., & Marshall, C. T. (2015). Resilience and tipping points of an exploited fish population  
 758 over six decades. *Global Change Biology*, 21(5), 1834–1847. doi:10.1111/gcb.12845
- 759 Verbesselt, J., Umlauf, N., Hirota, M., Holmgren, M., Van Nes, E. H., Herold, M., ... Scheffer, M. (2016). Re-  
 760 motely sensed resilience of tropical forests. *Nature Climate Change*, 1(September). doi:10.1038/nclimate3108
- 761 Villa Martín, P., Bonachela, J. A., & Muñoz, M. A. (2014). Quenched disorder forbids discontinuous  
 762 transitions in nonequilibrium low-dimensional systems. *Physical Review E*, 89(1), 12145. Retrieved from  
 763 <https://link.aps.org/doi/10.1103/PhysRevE.89.012145>
- 764 Villa Martín, P., Bonachela, J. A., Levin, S. A., & Muñoz, M. A. (2015). Eluding catastrophic shifts.  
 765 *Proceedings of the National Academy of Sciences*, 112(15), E1828–E1836. doi:10.1073/pnas.1414708112
- 766 Viña, A., McConnell, W. J., Yang, H., Xu, Z., & Liu, J. (2016). Effects of conservation policy on China's  
 767 forest recovery. *Science Advances*, 2(3), e1500965. Retrieved from <http://advances.sciencemag.org/content/2/3/e1500965.abstract>
- 768  
 769 Vuong, Q. H. (1989). Likelihood Ratio Tests for Model Selection and Non-Nested Hypotheses. *Econometrica*,  
 770 57(2), 307–333. doi:10.2307/1912557
- 771 Weerman, E. J., Van Belzen, J., Rietkerk, M., Temmerman, S., Kéfi, S., Herman, P. M. J., & Koppell, J. V.

- 772 de. (2012). Changes in diatom patch-size distribution and degradation in a spatially self-organized intertidal  
773 mudflat ecosystem. *Ecology*, 93(3), 608–618. doi:10.1890/11-0625.1
- 774 Weissmann, H., & Shnerb, N. M. (2016). Predicting catastrophic shifts. *Journal of Theoretical Biology*, 397,  
775 128–134. doi:10.1016/j.jtbi.2016.02.033
- 776 Wuyts, B., Champneys, A. R., & House, J. I. (2017). Amazonian forest-savanna bistability and human  
777 impact. *Nature Communications*, 8(May), 15519. doi:10.1038/ncomms15519
- 778 Xu, C., Hantson, S., Holmgren, M., Nes, E. H. van, Staal, A., & Scheffer, M. (2016). Remotely sensed  
779 canopy height reveals three pantropical ecosystem states. *Ecology*, 97(9), 2518–2521. doi:10.1002/ecy.1470
- 780 Zhang, J. Y., Wang, Y., Zhao, X., Xie, G., & Zhang, T. (2005). Grassland recovery by protection from  
781 grazing in a semi-arid sandy region of northern China. *New Zealand Journal of Agricultural Research*, 48(2),  
782 277–284. doi:10.1080/00288233.2005.9513657
- 783 Zinck, R. D., & Grimm, V. (2009). Unifying wildfire models from ecology and statistical physics. *The  
784 American Naturalist*, 174(5), E170–85. doi:10.1086/605959